ARTICLE

Fully Solution-Processed Inverted Polymer Solar Cells with Laminated Nanowire Electrodes

Whitney Gaynor,[†] Jung-Yong Lee,[‡] and Peter Peumans[‡,*]

[†]Department of Materials Science and Engineering and [‡]Department of Electrical Engineering, Stanford University, Stanford, California 94305

ABSTRACT We demonstrate organic photovoltaic cells in which every layer is deposited by solution processing on opaque metal substrates, with efficiencies similar to those obtained in conventional device structures on transparent substrates. The device architecture is enabled by solution-processed, laminated silver nanowire films serving as the top transparent anode. The cells are based on the regioregular poly(3-hexylthiophene) and C_{61} butyric acid methyl ester bulk heterojunction and reach an efficiency of 2.5% under 100 mW/cm^2 of AM 1.5G illumination. The metal substrates are adequate barriers to moisture and oxygen, in contrast to transparent plastics that have previously been used, giving rise to the possibility of roll-to-roll solution-processed solar cells that are packaged by lamination to glass substrates, combining the cost advantage of roll-to-roll processing with the barrier properties of glass and metal foil.

KEYWORDS: solution processing · transparent conductor · silver nanowires · organic photovoltaics

Organic bulk heterojunction photovoltaic (PV) cells fabricated from both polymers[1] and small molecules[2] show promise as an alternative to their inorganic counterparts with a potentially lower module cost per peak watt. Much of this cost reduction relies on the ability to use high-throughput processing techniques such as roll-to-roll coating on low-cost substrates. Both vacuum and solution-based roll-to-roll coating can be cost-effective, and the lowest costs will be achieved when all coating steps are performed either from solution or in vacuum as this prevents the need to switch between tools. Metal foil substrates and plastic foils with opaque metal coatings are particularly attractive because they are low-cost and, unlike transparent plastic foil substrates, have excellent barrier properties against the permeation of O_2 and H_2O, which would otherwise lead to device degradation.[3−5] However, no high-performance polymer devices whose active layer is deposited from solution onto metal foil without the use of vacuum deposition for some of the layers have been reported. The goal of this work is three-fold: (1) to develop a device that can be processed onto a substrate using only solution processes, (2) to eliminate the costly metal oxide transparent electrode and replace it with an equivalent that is solution-processed and equally conductive and transparent, and (3) to invert the devices optically such that light is not incident from the substrate side to allow for the use of opaque metal substrates with good barrier properties.

The organic bulk heterojunction system used here consists of the donor material regioregular poly(3-hexylthiophene) (P3HT) and the fullerene derivative [6,6]phenyl C_{61} butyric acid methyl ester (PCBM). This system has produced single-junction cell efficiencies over 4%.[6−8] The most common device of this type is fabricated using the superstrate cell structure: glass/indium tin oxide (ITO)/poly(4,3-ethylene dioxythiophene) (PEDOT):poly(styrene sulfonate) (PSS)/P3HT:PCBM/Al. Often, a thin evaporated layer of LiF or another alkali metal containing salt is added between the polymer and Al cathode to lower the barrier to electron transport at that interface.[9] More recently, polymer bulk heterojunction devices have been reported that are electrically inverted.[10−16] The ITO-coated glass or plastic is still the superstrate, but in these devices, the ITO functions as the cathode. To change the workfunction of the ITO, various strategies have been used, such as treatment with Cs_2CO_3 using vacuum deposition[10] and solution processing,[11,12] solution-processed amorphous TiO_x[13−15] and ZnO,[16] and self-assembled monolayers.[17] These devices have reached power conversion efficiencies over 4%.[11]

However, there remain problems with this approach. Indium is an expensive

*Address correspondence to ppeumans@stanford.edu.

Received for review July 7, 2009 and accepted December 15, 2009.

Published online December 21, 2009. 10.1021/nn900758e

metal, and ITO is deposited in a time-consuming sputtering process, which would damage the underlying organic if used as a top electrode.[18] In addition, the brittle nature of ITO makes it unattractive for use in flexible organic solar cells.[19] Various solution-processable alternatives to ITO have been proposed and used in solar cells, including carbon nanotubes (CNTs)[20−22] and graphene sheets,[23−26] and more recently combinations thereof.[27] Even though reasonable device efficiencies have been obtained in organic PV cells in which ITO was replaced with CNTs in the standard device configuration,[21] the properties of CNT films do not compare favorably to ITO. The sheet resistances are around 200 Ω/□ at the 85−90% transmissivity required for efficient device performance.[20,21] The only polymer bulk heterojunction device reported in which a CNT film was used as a top electrode in an inverted organic PV cell on ITO yielded a poor power conversion efficiency of 0.3%.[22] Graphene sheets show similar performance to CNT films and in addition require very high temperature annealing steps to obtain conductivities that are still too low for efficient devices to be fabricated.[25,26] Combining the two carbon nanostructures into one electrode still does not result in sheet resistivities and transmissivities comparable to ITO.[27] Ag nanowire films remain the only solution-deposited ITO alternative that meets the performance requirements for photovoltaics, at 10 Ω/□ with 85% transmissivity over the wavelength from 400 to 800 nm,[28] and in this paper, we demonstrate their use as a top electrode.

A few previous organic solar cell device architectures that are ITO-free have been reported, with the layers deposited in a substrate configuration onto metal. One structure showed poor device performance using monochromatic light.[29] Another utilizes e-beam evaporated Ti as the cathode and a shadow-masked evaporated Ag grid for the anode, which shades part of the device area, lowering device performance.[30] Semitransparent metal films have been used as transparent top electrode in vacuum-deposited small-molecule devices on metal substrates.[31−33] No device has been reported in which every layer is deposited from solution onto a low-cost substrate with good barrier properties to yield promising device efficiencies. Here, we fabricate an efficient P3HT:PBCM bulk heterojunction organic solar cell on a metal substrate with the active layer, workfunction adjustment layers, and transparent electrode all deposited from solution.

RESULTS AND DISCUSSION

Fully solution-processed devices on opaque silver substrates are fabricated in two parts: the lower device layers, which are spin-cast, and the top transparent anode, which is laminated onto the device. Figure 1a shows the device structure and a diagram of the lamination process. Cs_2CO_3, spin-cast from solution, is used to reduce the Ag cathode workfunction as described by

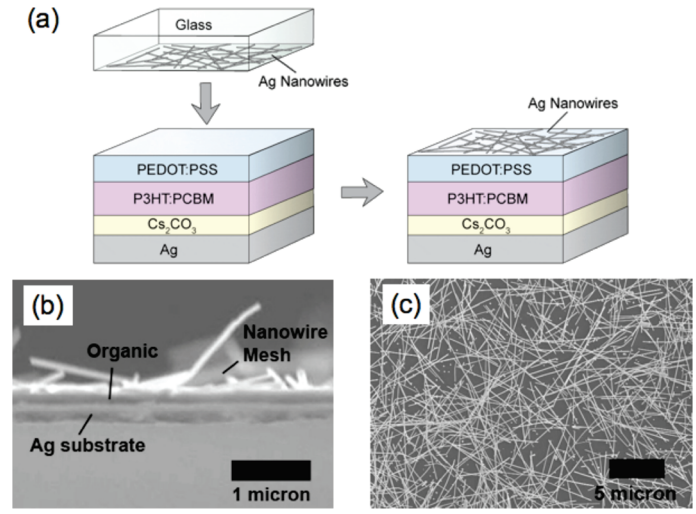

Figure 1. (a) Device structure and lamination process. All layers below the nanowires are deposited by spin-casting onto the Ag substrate. (b) Cross-sectional scanning electron micrograph (SEM) in which the Ag film, the organic layers, and the top Ag nanowire mesh electrode are visible. Nanowires sunk into and adhered to the organic layer can be seen at that interface. (c) Top-view SEM of the devices in which the nanowire mesh is shown to be a continuous network.

Liao *et al.*[11] This is followed by the spin-cast P3HT:PCBM blend, and finally, the PEDOT:PSS is spun on top of the bulk heterojunction layer. Prior to spinning, the PEDOT:PSS is sonicated for 15 min and then heated at 90 °C for 25 min.[34] This approach improves wetting of the hydrophobic P3HT:PCBM by the hydrophilic PEDOT:PSS. In this way, each device layer is deposited from solution onto the primary substrate.

The top electrode (anode) is fabricated from a Ag nanowire mesh. Ag nanowire electrodes have been shown to have a transparency similar to ITO at a sheet resistance of ∼10 Ω/□, appropriate for use in thin-film photovoltaics.[28] Prior to lamination, the Ag nanowire films are pressed with a clean glass substrate to flatten the nanowire mesh and remove features that may otherwise punch through the active layer. The pressed films are then laminated on top of the PEDOT:PSS surface of the solar cell structures, as shown in Figure 1a. In a manufacturing process, this step could serve to both complete the devices and package them, leaving them between two low-cost, highly protective barrier layers, glass and metal. This would eliminate the need for additional packaging steps and materials, driving down manufacturing cost. In this case, for laboratory devices, the glass donor substrate is removed to leave the nanowires transferred to the PEDOT:PSS as the top electrode. The nanowires sink into the soft polymer layer and adhere, as is visible at the organic−nanowire interface in the cross-sectional scanning electron micrograph (SEM) in Figure 1b. However, some portions of the nanowires also lift up as the glass is removed, which is also clearly visible in this micrograph. An SEM of the top surface of the finished devices is shown in Figure 1c. The Ag nanowires form a continuous mesh over the de-

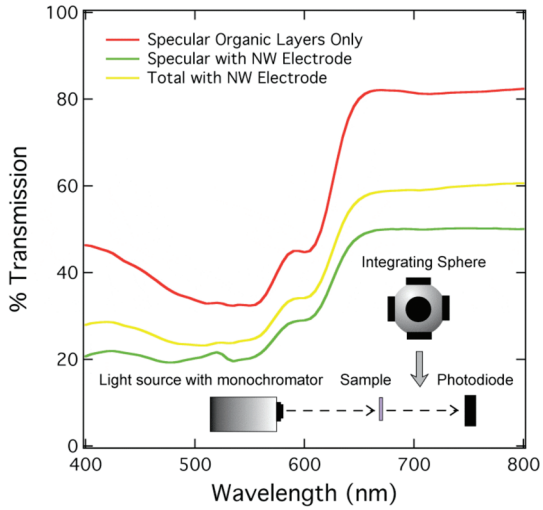

Figure 2. Specular transmission over the range of visible wavelengths for the organic layers used in the device with (green) and without (red) the top Ag nanowire mesh electrode. Total (specular plus diffuse) transmission over the range of visible wavelengths for the organic layers with the top Ag nanowire mesh electrode (yellow).

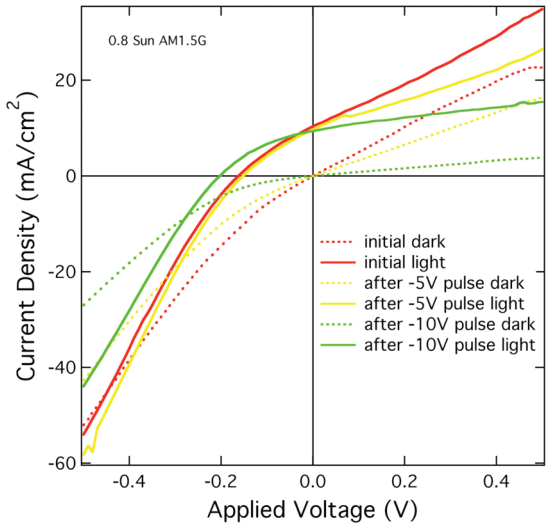

Figure 3. Current density−voltage (*J*−*V*) curves for non-optimized devices measured as-fabricated (red), following millisecond pulsing at −5 V (yellow), and at −10 V (green) in the dark (dashed lines) and under 80 mW/cm^2 AM 1.5G illumination (solid lines).

vice surface through which current can be conducted laterally.

Figure 2 shows specular optical transmission data over visible wavelengths for a device structure without the Ag/Cs_2CO_3 cathode, deposited on quartz both with (green) and without (red) a nanowire anode. Also shown is total optical transmission data collected using an integrating sphere (yellow) for the same structure with the anode. The specular transmittance through the device decreases when the nanowires are present due to both optical absorption in the nanowires and due to scattering. The total transmission curve includes the light scattered through the device by the nanowires. By comparing the total and specular curves for the structures with nanowires and averaging over the visible spectrum, it is shown that 83% of the transmission through the Ag nanowire mesh is specular and the remaining 17% is diffuse. This plot also shows that, in the wavelength region from 450 to 650 nm, where the absorption of the active layer is the strongest, the decrease in total transmission due to the nanowires averages only 11.8%, resulting in a total transmissivity of 88.2% through the nanowires in this region. Over the entire visible spectrum, this loss is 16.2%, resulting in a total transmissivity of 83.8%. Both of these numbers are consistent with previous reports for the solar transmittance of Ag nanowire meshes with conductivities useful for photovoltaics.[28]

When *J*−*V* curves for these devices were measured in the dark and under illumination, large dark leakage currents were observed. Figure 3 shows non-optimized *J*−*V* device data for these devices as fabricated (red) in the dark (dashed line) and under 80 mW/cm^2 of AM 1.5G illumination (solid line). The large dark currents are attributed to the roughness of the nanowire electrode, which results in some nanowires extending further into the active layer and creating locally thinned device regions. These preferential current pathways can be eliminated by applying millisecond long voltage pulses in forward bias to burn local shorts. Figure 3 also shows *J*−*V* curves in the dark (dashed lines) and under illumination (solid lines) following an applied pulse of −5 V (yellow) and −10 V (green).

J−*V* curves in the dark (green dashed line) and under 100 mW/cm^2 AM 1.5G illumination (green solid line) are shown in Figure 4. For the device structure described above, with a device area of 2 mm^2, the open circuit voltage is V_{OC} = 0.51 V, the short circuit current

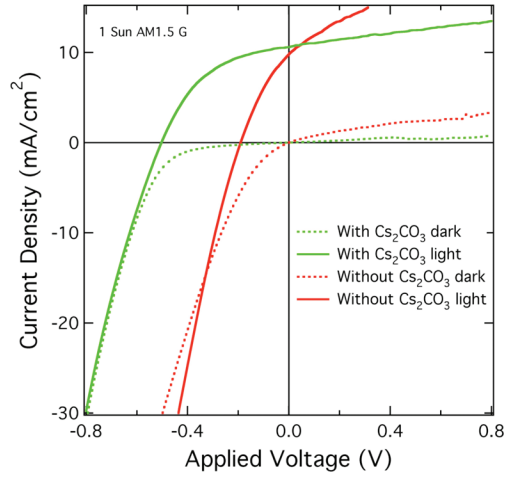

Figure 4. Current density−voltage (*J*−*V*) characteristics for the partially optimized organic PV cells in the dark (dashed lines) and under 100 mW/cm^2 AM 1.5G illumination (solid lines). The green curves are for a device with the structure Ag/Cs_2CO_3/P3HT:PCBM/PEDOT/Ag nanowire mesh. The red curves are for the same device structure, omitting the Cs_2CO_3 interface layer.

density is $J_{SC} = 10.59$ mA/cm^2, and the fill factor is 0.46. This yields a power conversion efficiency of $\eta = 2.5\%$. These devices retain some conduction through a shunt, as seen in the dark $J-V$ characteristics. This is attributed to the remaining roughness of the nanowire electrode and the resulting locally thinned device regions, which produce a shunt resistance of 1 kΩ/cm^2. The V_{OC} of these devices is around 100 mV lower than the best devices made in the standard configuration.[6−8] This may be partially due to the lack of chemical or structural modifications that occur when the metal cathode is evaporated onto the polymer in superstrate devices.[35] This alters the barrier to charge transport at this interface and could play a role in lowering the V_{OC}.

Also shown in Figure 4 are the $J-V$ characteristics of a device without the Cs_2CO_3 treatment of the Ag cathode in the dark (dashed red line) and under illumination (solid red line). V_{OC} is reduced to 0.19 V, J_{SC} to 7.8 mA/cm^2, and the fill factor to 0.32, resulting in a power conversion efficiency of $\eta = 0.6\%$. The increase in leakage current originates from the use of a thicker, nonoptimized nanowire electrode in this device. These results show that the Cs_2CO_3 layer enhances charge collection and transport between the Ag substrate and the organic layers. This is consistent with reported findings for both solution-processed and evaporated Cs_2CO_3 interface layers, which have been found to lower the Ag workfunction to 3.45 eV (spin-cast Cs_2CO_3), 3.06 eV (spin-cast Cs_2CO_3 after annealing),[11] and 2.2 eV (vacuum-deposited Cs_2CO_3).[10]

CONCLUSIONS

In summary, we report fully solution-processed organic photovoltaic cells that are electrically and optically inverted on opaque Ag cathodes. This device structure is made possible through the use of laminated Ag nanowire meshes as the top transparent conducting electrode. These electrodes are currently the only solution-processed ITO alternative that has a performance comparable to sputtered transparent conducting oxides, and in this work, we demonstrate their transfer and use as top electrodes. The fabricated PV cells reach a power conversion efficiency of 2.5% under 100 mW/cm^2 of AM 1.5G illumination, and because they are deposited onto metal, they have unique advantages. Metals are exceptional barriers to moisture and oxygen,[3] and they can be textured or shaped into different form factors to enhance light trapping.[36,37] Hermetic cell packaging can be achieved by laminating these cells to glass. Such an approach retains the throughput advantages of roll-to-roll deposition but uses glass substrates as a barrier and convenient form factor for panel installation. These cells are also potentially useful as components in tandem cells that are not constrained by current matching. Because they are ITO-free and fully processed from solution, their cost is potentially very low.

EXPERIMENTAL SECTION

Device Preparation. All device preparation steps are carried out in a nitrogen glovebox. The PV cells are built on an opaque 150 nm thick vacuum-deposited, patterned Ag film on precleaned glass. The glass substrate is not essential but provides a convenient way to handle the substrates during the subsequent spin-coating steps. Cs_2CO_3 (Aldrich) in 0.2 wt % 2-ethoxyethanol solution is spun onto the Ag film and then annealed for 20 min on a hot plate at 150 °C to reduce the cathode workfunction.[11] Samples for XPS are completed after this step and removed from the glovebox for measurement. For photovoltaic cells, the Cs_2CO_3 layer is followed by spinning on a 2.5 wt % 1:1 P3HT (Rieke Metals, Inc.):PCBM (Nano-C, Inc.) blend from *ortho*-dichlorobenzene at 600 rpm for 45 s. The films are allowed to dry in a covered Petri dish and are then annealed at 110 °C for 10 min to evaporate remaining solvent. The PEDOT:PSS (Clevios CPP 105D, H.C. Starck) is sonicated for 15 min and heated at 90 °C for 25 min[34] and is then spun on top of the bulk heterojunction layer. The device is then annealed at 130 °C for 25 min, which smoothes the PEDOT:PSS surface and evaporates water left in the film.

Electrode Fabrication. The Ag nanowire mesh is prepared on a separate precleaned glass substrate by drop-casting a suspension of Ag nanowires and allowing them to dry while agitated on a shaker.[28] The glass is dipped in an aqueous poly-L-lysine solution (0.1% w/v, Ted Pella) for 5 min prior to coating to increase its affinity for the nanowires. The mesh films are then annealed at 180 °C for 1 h to lower the sheet resistance.[28] The as-prepared Ag nanowire films are pressed with a clean glass substrate at 5.9 × 10^3 psi for 30 s to flatten the nanowire mesh. The pressed films are then laminated on top of the PEDOT:PSS surface of the solar cell structures under the same pressure for 1 min. The glass donor substrate is removed to leave the nanowires transferred to the PEDOT:PSS as the top electrode.

Electrical Measurements. For current density−voltage ($J-V$) measurements, the bottom Ag anode is exposed by dissolving the nanowires and polymer layers with acetone, while the nanowire electrode is contacted on top with a soft probe consisting of a fine (100 μm diameter) Au wire. The Ag cathode is contacted with a hard probe. $J-V$ measurements are conducted in air in the dark and under 100 mW/cm^2 of AM 1.5G illumination, using an Agilent 1455 C semiconductor parameter analyzer. We note that no spectral correction factor was used to correct J_{SC} and η.

Optical Measurements. Specular transmission measurements are taken using a white light source with a monochromator and a silicon photodiode (Newport Corporation). An integrating sphere is placed between the sample and the photodiode for total (specular plus diffuse) transmission measurements.

Acknowledgment. The authors thank H.S. Kim and Y. Cui for providing silver nanowires. This work was supported by the Center for Advanced Molecular Photovoltaics (Award No KUS-C1-015-21), made by King Abdullah University of Science and Technology (KAUST), and the Global Climate and Energy Project at Stanford.

REFERENCES AND NOTES

1. Brabec, C. J.; Sariciftci, N. S.; Hummelen, J. C. Plastic Solar Cells. *Adv. Funct. Mater.* **2001**, *11*, 15–26.
2. Peumans, P.; Uchida, S.; Forrest, S. Efficient Bulk Heterojunction Photovoltaic Cells Using Small-Molecular-Weight Organic Thin Films. *Nature* **2003**, *425*, 158–162.
3. Treutlein, R.; Bergsmann, M.; Stonley, C. J. Reel-to-Reel Vacuum Metallization. In *Organic Electronics, Materials, Manufacturing and Applications*; Klauk, H., Ed.; Wiley-VCH

Verlag GmbH & Co. KGaA: Weinheim, Germany, 2006; pp 183−202.
4. Günes, S.; Neugebauer, H.; Sariciftci, N. S. Conjugated Polymer-Based Organic Solar Cells. *Chem. Rev.* **2007**, *107*, 1324–1338.
5. Jorgensen, M.; Normann, K.; Krebs, F. C. Stability/Degradation of Polymer Solar Cells. *Sol. Energy Mater. Sol. Cells* **2008**, *92*, 686–714.
6. Li, G.; Shrotriya, V.; Yao, Y.; Yang, Y. Investigation of Annealing Effects and Film Thickness Dependence of Polymer Solar Cells Based on Poly(3-hexylthiophene). *J. Appl. Phys.* **2005**, *98*, 043704-5.
7. Li, G.; Shrotriya, V.; Huang, J.; Yao, Y.; Moriarty, T.; Emery, K.; Yang, Y. High-Efficiency Solution Processable Polymer Photovoltaic Cells by Self-Organization of Polymer Blends. *Nat. Mater.* **2005**, *4*, 864–868.
8. Kim, Y.; Cook, S.; Tuladhar, S. M.; Choulis, S. A.; Nelson, J.; Durrant, J. R.; Bradley, D. D. C.; Giles, M.; McCulloch, I.; Ha, C. S.; Ree., M. A. Strong Regioregularity Effect in Self-Organizing Conjugated Polymer Films and High-Efficiency Polythiophene:Fullerene Solar Cells. *Nat. Mater.* **2006**, *5*, 197–203.
9. Shaheen, S.; Brabec, C. J.; Sariciftci, N. S.; Padinger, F.; Fromherz, T.; Hummelen, J. 2.5% Efficient Organic Plastic Solar Cells. *Appl. Phys. Lett.* **2001**, *78*, 841–843.
10. Li, G.; Chu, C.-W.; Shrotriya, V.; Huang, J.; Yang, Y. Efficient Inverted Polymer Solar Cells. *Appl. Phys. Lett.* **2006**, *88*, 253503-3.
11. Liao, H.; Chen, L.; Xu, Z.; Li, G.; Yang, Y. Highly Efficient Inverted Polymer Solar Cell by Low Temperature Annealing of Cs_2CO_3 Interlayer. *Appl. Phys. Lett.* **2008**, *92*, 173303-3.
12. Huang, J; Li, G.; Yang, Y. A. Semi-transparent Plastic Solar Cell Fabricated by a Lamination Process. *Adv. Mater.* **2008**, *20*, 415–419.
13. Waldauf, C.; Morana, M.; Denk, P.; Schilinsky, P.; Coakley, K.; Choulis, S. A.; Brabec, C. J. Highly Efficient Inverted Organic Photovoltaics Using Solution Based Titanium Oxide as Electron Selective Contact. *Appl. Phys. Lett.* **2006**, *89*, 233517-3.
14. Kuwabara, T.; Nakayama, T.; Uozumi, K.; Yamaguchi, T.; Takahashi, K. Highly Durable Inverted-Type Organic Solar Cell Using Amorphous Titanium Oxide as Electron Collection Electrode Inserted Between ITO and Organic Layer. *Sol. Energy Mater. Sol. C* **2008**, *92*, 1476–1482.
15. Seim, R.; Choulis, S. A.; Schilinsky, P.; Brabec, C. J. Interface Modification for Highly Efficient Organic Photovoltaics. *Appl. Phys. Lett.* **2008**, *92*, 093303-3.
16. White, M. S.; Olson, D. C.; Shaheen, S. E.; Kopikakis, N.; Ginley, D. S. Inverted Bulk-Heterojunction Organic Photovoltaic Device Using a Solution-Derived ZnO Underlayer. *Appl. Phys. Lett.* **2006**, *89*, 143517-3.
17. Kim, J.; Khang, D. Y.; Kim, J. H.; Lee, H. H. The Surface Engineering of Top Electrode in Inverted Polymer Bulk-Heterojunction Solar Cells. *Appl. Phys. Lett.* **2008**, *92*, 133307-3.
18. Zweibel, K. Thin Film PV Manufacturing: Materials Costs and Their Optimization. *Sol. Energy Mater. Sol. C* **2000**, *63*, 375–386.
19. Park, S. K.; Han, J. I.; Moon, D. G.; Kim, W. K. Mechanical Stability of Externally Deformed Indium-Tin-Oxide Films on Polymer Substrates. *Jpn. J. Appl. Phys.* **2003**, *42*, 623–629.
20. Du Pasquier, A.; Unalan, H. E.; Kanwal, A.; Miller, S.; Chhowalla, M. Conducting and Transparent Single-Wall Carbon Nanotube Electrodes for Polymer-Fullerene Solar Cells. *Appl. Phys. Lett.* **2005**, *87*, 203511-3.
21. Rowell, M. W.; Topinka, M. A.; McGehee, M. D.; Prall, H. J.; Dennler, G.; Saricifti, N. S.; Hu, L.; Gruner, G. Organic Solar Cells With Carbon Nanotube Network Electrodes. *Appl. Phys. Lett.* **2006**, *88*, 233506-3.
22. Tanaka, S.; Mielczarek, K.; Ovalle-Robles, R.; Wang, B.; Hsu, D.; Zahkidov, A. A. Monolithic Parallel Tandem Organic Photovoltaic Cell with Transparent Carbon Nanotube Interlayer. *Appl. Phys. Lett.* **2009**, *94*, 113506-3.
23. Eda, G.; Fanchini, G.; Chhowalla, M. Large-Area Ultrathin Films of Reduced Graphene Oxide as a Transparent and Flexible Electronic Material. *Nat. Nanotechnol.* **2008**, *3*, 270–274.
24. Becerril, H. A.; Mao, J.; Liu, Z.; Stoltenberg, R. M.; Bao, Z.; Chen, Y. Evaluation of Solution-Processed Reduced Graphene Oxide Films as Transparent Conductors. *ACS Nano* **2008**, *2*, 463–470.
25. Wang, X.; Zhi, L.; Müllen, K. Transparent, Conductive Graphene Electrodes for Dye-Sensitized Solar Cells. *Nano Lett.* **2008**, *8*, 323–327.
26. Wu, J.; Becerril, H. A.; Bao, Z.; Liu, Z.; Chen, Y., P. Peumans, Organic Solar Cells with Solution-Processed Graphene Transparent Electrodes. *Appl. Phys. Lett.* **2008**, *92*, 263302-3.
27. Tung, V. C.; Chen, L. M.; Allen, M. J.; Wassei, J. K.; Nelson, K.; Kraner, R. B.; Yang, Y. Low-Temperature Solution Processing of Graphene-Carbon Nanotube Hybrid Materials for High-Performance Transparent Conductors. *Nano Lett.* **2009**, *9*, 1949–1955.
28. Lee, J. Y.; Connor, S. T.; Cui, Y.; Peumans, P. Solution-Processed Metal Nanowire Mesh Transparent Electrodes. *Nano Lett.* **2008**, *8*, 689–692.
29. Nyberg, T. An Alternative Method to Build Organic Photodiodes. *Synth. Met.* **2004**, *140*, 281–286.
30. Glatthaar, M.; Niggemann, M.; Zimmermann, B.; Lewer, P.; Riede, M.; Hinsch, A.; Luther, J. Organic Solar Cells Using Inverted Layer Sequence. *Thin Solid Films* **2005**, *491*, 298–300.
31. Pode, R. B.; Lee, C. J.; Moon, D. G.; Han, J. I. Transparent Conducting Metal Electrode for Top Emission Organic Light-Emitting Devices: Ca-Ag Double Layer. *Appl. Phys. Lett.* **2004**, *84*, 4614–4616.
32. Meiss, J.; Allinger, N.; Riede, M. K.; Leo, K. Improved Light Harvesting in Tin-Doped Indum Oxide (ITO)-Free Inverted Bulk-Heterojunction Organic Solar Cells Using Capping Layers. *Appl. Phys. Lett.* **2008**, *93*, 103311-3.
33. O'Connor, B.; Pipe, K. P.; Shtein, M. Fiber Based Organic Photovoltaic Devices. *Appl. Phys. Lett.* **2008**, *92*, 193306-3.
34. Ravirajan, P.; Bradley, D. D. C.; Nelson, J.; Haque, S. A.; Durant, J. R.; Smit, H. J. P.; Kroon, J. M. Efficient Charge Collection in Hybrid Polymer/TiO_2 Solar Cells Using Poly(ethylenedioxythiophene)/Polystyrene Sulphonate as Hole Collector. *Appl. Phys. Lett.* **2005**, *86*, 143101-3.
35. Ishii, H.; Sugiyama, K.; Ito, E.; Seki, K. Energy Level Alignment and Interfacial Electronic Structures at Organic/Metal and Organic/Organic Interfaces. *Adv. Mater.* **1999**, *11*, 605–625.
36. Rim, S. B.; Zhao, S.; Scully, S. R.; McGehee, M. D.; Peumans, P. An Effective Light Trapping Configuration for Thin-Film Solar Cells. *Appl. Phys. Lett.* **2007**, *91*, 243501-3.
37. Tvingstedt, K.; Andersson, V.; Zhang, F.; Inganas, O. Folded Reflective Tandem Polymer Solar Cell Doubles Efficiency. *Appl. Phys. Lett.* **2007**, *91*, 123514-3.